Improved scheme of membership function optimisation for fuzzy air-fuel ratio control of GDI engines

Li, Ji; Li, Ziyang; Zhou, Quan; Zhang, Yunfan; Xu, Hongming

DOI:
10.1049/iet-its.2018.5013

An Improved Scheme of Membership Function Optimisation for Fuzzy Air-fuel Ratio Control of GDI engines

Ji Li[1], Ziyang Li[1], Quan Zhou[1], Yunfan Zhang[1], Hongming Xu[1] ✉

[1] Department of Mechanical Engineering, School of Engineering, University of Birmingham, B15 2TT, UK
✉ E-mail: h.m.xu@bham.ac.uk

Abstract: This paper researches an improved scheme of Membership Function Optimisation (MFO) for fuzzy Air-fuel Ratio (AFR) control of Gasoline Direct Injection (GDI) engines based on Correspondence Analysis (CA). This PI-like Fuzzy Knowledge-Based Controller (FKBC) optimised by the proposed scheme can further optimise AFR control performance while maximising conversion efficiency of the Three-Way Catalyst (TWC) to eliminate the exhaust emissions in real-time. Different from the conventional experience-based Membership Function Design (MFD) method for an FKBC, the proposed MFO scheme uses CA approach and can visualise the relationship between engine step gain scenarios and designed MF patterns to precisely determine its scalar parameters for AFR regulation of GDI engines. Within this context: 1) Specialised MFs for self-adaptive AFR control system of a GDI engine are designed with weight distribution. 2) Based on designed scalar parameters, the CA model with taxonomic dimensions is built for acquiring a customised MF to counter transient scenario changes more effectively. 3) The engine controller with the proposed scheme is real-time validated in a production V6 GDI engine, and its advantage in terms of engine transient control performance is further demonstrated by comparing with a benchmark controller designed based on experience.

1. Introduction

Currently, emissions of nitrogen oxides, total hydrocarbon, non-methane hydrocarbons, carbon monoxide and particulate matter are regulated for most vehicle types. To develop the automotive fuel economy globally, European emission standards VI has been proposed in 2014 as part of the EU framework for regulating each type approval of vehicles strictly [1]. Compared to the conventional non-diesel injection process, the gasoline is injected into the cylinder directly with the in-cylinder flow and fuel atomization on the piston surface as the gas mixture for combustion [2]. Main technical features of GDI engines are the ultra-thin combustion and direct injection, which can decrease the brake specific fuel consumption and intake resistance respectively [3]. Specifically, AFR of GDI engine can reach 40: 1 with lean combustion technology, the maximum up to 100: 1, which could enhance the robustness, transient response and decrease the detonation tendency emission [4].

Advanced engine control technologies are engaged because of the strict emission regulations and demand for higher fuel economy [5]. Control has always been a part of engine design and it is one of the most complex problems in the application [6]. Generally, IC engines use model-based proportional–integral–derivative (PID) closed-loop control system to maximise engine's dynamic and economic performances at different working conditions [7]. Fundamental difficulties with PID control one is that it is a feedback control system, with constant parameters, and no direct knowledge of the process, and thus overall performance is reactive and a compromise. The other is model-based control systems are unable to revise errors of unknown calibration points [8]. Recently, some literature has proposed real-time simulation models to manage the AFR fluctuation by [9]-[11], actually, they cannot prove the contribution of the real engine practice due to much more complex operation conditions. In 2014, Denis V. presented a supervisory control system switching between two control laws to improve quality of the closed-loop system [12]. Relatively, to construct two control laws need to spend huge workload on identifying engine model. In 2016, Madan K. pointed out that a cyclic model based generalized predictive control of AFR for V6 GDI engines [13], which shows reflect the cycle-to-cycle coupling effects of residual gas mass.

Actually, it is hard to predict the nonlinear relation of the model-based controller and the transient response performance is not optimistic as results.

To overcome uncertainties to non-calibration points and to reduce consumptions of time and experience, researchers increasingly utilise fuzzy logic algorithms to optimise industrial issues. Riccardo B. presented a systematic MFD of a Fuzzy Logic Controller (FLC) to simplify decision procedure with multivariable in the biological system [14]. Christian A. demonstrated a predictive torque controller for an induction motor drive to replaces the minimization of a scalar cost function with fuzzy decision-making [15]. Nabipour, M. indicated using computationally-light algorithm to tuning fuzzy membership function for a PV-based dynamic voltage restorer, whereas this algorithm complexity increases consumptions of time and experience and have not been able to achieve in engineering practice [16]. Sicre, C. purposed real-time regulation of efficient driving of high speed trains [17], comparing to engine systems, its dynamic model takes advantages of less influencing factors and weak disturbance. The foregoing papers only focus on non-transient or linear conditions, which never appear particularly in engine practice. Obviously, the literature is quite deficient that involves using fuzzy control strategy on the optimisation of GDI engine performance. With considerations of nonlinear transient circumstances, some papers have introduced advanced algorithms [18], [19] to improve vehicle performance, and [20]-[24] optimised fuzzy logic controllers with intelligent calibration.

Our previous work [25]-[28] shows although GDI engines performance can be improved through intelligent calibration, their transient behaviours cannot be easily described

quantitatively and the adaptability of its control system needs to be improved. To develop robustness of the engine control system, so far an FLC has been introduced with direct methods drawing on expert knowledge to provide fuzzy set membership scores [9][10]. The mismatch between engine fuel injection and mass air flow is dominating factor to the spikes of AFR trajectory and the deteriorated engine emissions [8]. As shown in Fig. 1, the fuzzy controlled AFR trajectory has the lower overshooting and the shorter convergence time compared with the PI controlled AFR trajectory, which proved by [10]-[12], [27]. This paper aims at further improving the accuracy of AFR control in GDI engines during the transient scenario in order to reduce the emissions caused by perturbation of AFR. The proposed MFO scheme uses CA approach to visualise descriptive statistics of relations between fuzzy sets, which determines MF scalar parameter of an FKBC for the GDI engine AFR control management. The customised MF with its homogenization can keep trend characteristics of designed MFs while repairing the insensitive interval.

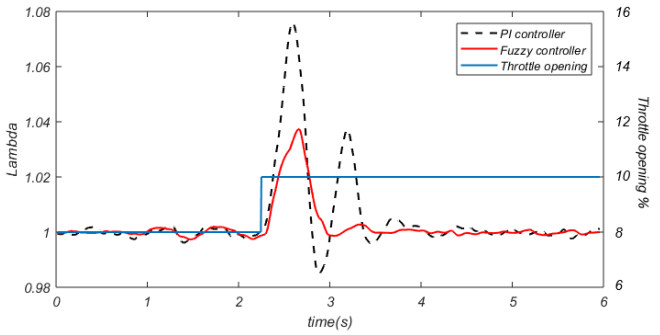

Fig. 1. *AFR transient response sample.*

The main work reported in this paper includes: 1) An FKBC framework is developed for self-adaptive AFR control system of the GDI engine. 2) Specialised MF is designed based on weight distribution, then the CA model with taxonomic dimensions is built for acquiring a customised MF to counter the transient scenarios changes more effectively. 3) Various transient circumstances encountered by different scenarios are considered to assess the CA-based MF pattern by means of studying their impact on behaviours of GDI engines. Therefore, a spectrum of comparisons with existing controllers is carried out to further demonstrate self-adaptive advantages of our approach.

The remainder of the paper proceeds as follows. The FKBC is introduced into AFR control system in Section II; the MFO scheme is presented with three main parts sequentially, followed by MFD, the establishment of analytical model in Section III, whereas it declares the Rapid Control Prototyping (RCP) control system and experimental setup with technical cores; Section IV organises CA result, MF suitability assessment and real-time comparative outcomes; conclusions are eventually summarised in Section V.

2. Description of Air-Fuel Ratio Control System

2.1. System Architecture

The architecture of the GDI engine considered in this study is given in Fig. 2. The main components include an air throttle, fuel injector, combustion chamber and Lambda sensor [29]. During working scenario changes with pedal tip-in, the air flow system directly influences the engine performance. The target AFR is used with the milligrams of air per cylinder to determine the desired fuel mass, which further defines the desired AFR for the engine based on operating state and sensor inputs to ensure the maximum conversion efficiency of the TWC.

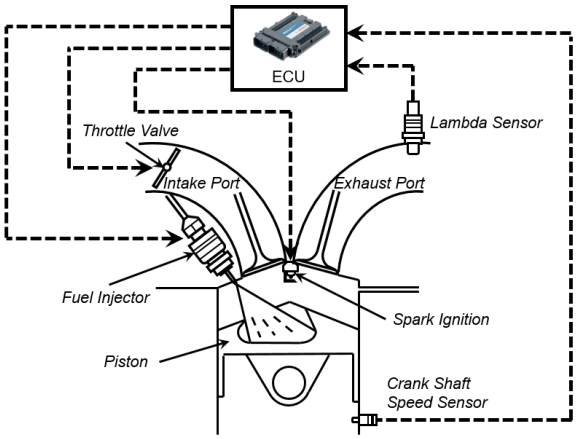

Fig. 2. *The schematic architecture of a GDI engine.*

2.2. PI-like Fuzzy Knowledge-Based Air-Fuel Ratio Controller

To realise the real-time AFR control model for GDI engines with fuzzy self-adaptive enhancement, this discrete control model has been promoted from Saraswati, S. [9] and Jansri, A. [10] as Fig. 3. AFR adjustment with a PI-like FKBC is determined by the required relative fuel mass compensation.

In the present approach, the PI system is a forward constraint for scaling input variables estimated from original engine calibration parameters. Based on the testing bench, the signal about actual AFR ($\overline{AFR}$) is calculated from a Lambda sensor. It is compared with the reference signal (AFR_{ref}) to generate an error signal. The nonlinear fuzzy logic approach has been chosen for the controller design due to highly nonlinear dynamics of the GDI engine. At the begin, let us consider a control action of a typical PI controller described in the frequency domain by

$$u_{PI}(k) = K_p \cdot e + K_I \cdot \sum \Delta e \qquad (1)$$

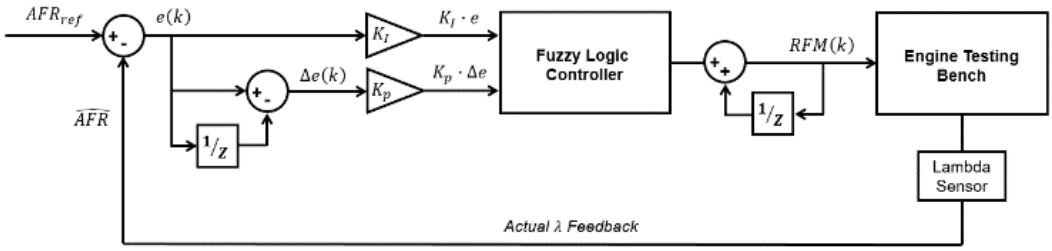

Fig. 3. *The working process for PI-like fuzzy controlled V6 Engine.*

Where K_p and K_i are the proportional and the integral gain coefficients. With derivative consideration**, Eq. (1)** is transformed into an equivalent expression

$$\Delta u_{PI}(k) = K_p \cdot \Delta e + K_I \cdot e \quad (2)$$

In this case, the rules database inputs and outputs are modelled as fuzzy variables. The error signal between the desired value of AFR (AFR_{ref}) and its actual AFR ($\widehat{AFR}$) obtained from the feedback of GDI engine bench, which is taken as one of the input and is given by

$$e(k) = AFR_{ref} - \widehat{AFR} \quad (3)$$

Further, change in error signal for two consecutive cycles is taken as other input and is given by

$$\Delta e(k) = e(k) - e(k-1) \quad (4)$$

Where $e(k-1)$ is error signal of the preceding cycle. Further, an output of the controller is the change in relative fuel mass $\Delta RFM(k)$. This is used to determine required relative fuel mass as given by

$$RFM(k) = RFM(k-1) + \Delta RFM(k) \quad (5)$$

Where $RFM(k-1)$ is the relative fuel mass of the preceding cycle.

The rules defined in rule base of the fuzzy logic controller are abstract ideas about how to achieve good control. To describe these ideas, inputs and output are described as linguistic variables. In this case, following linguistic variables are used:

'error' describes $e(k) \cdot K_i$
'change-in-error' describes $\Delta e(k) \cdot K_p$ *and*
'change-in-RFM' describes $\Delta RFM(k)$

The purpose of MFs is to map precise discrete values into continuous fuzzy variables. The subset division of fuzzy variables determines the number of rules. The number of rules should increase with refining the rule division. The linguistic quantification about two-inputs of *error* and Δ*error* defined on universes of discourse (U) then result in a 7×7 rules base for individuals in Table 1. The size of the term set determines the granularity of the control action in tabular form as [30] considered. For instance, one of rules is

If error is PM and change-in-error is NS, then change-in-relative fuel mass is PS.

Where *PM, NS* and *PS* are fuzzy sets, defined on universes of discourse (domains) *E*, change of $\dot{E}$ and $\dot{U}$ respectively. The ternary fuzzy relation *R* defined as often represents this rule:

$$R = \int_{E \times \Delta E \times \Delta U} \min\left(\mu_{PM}(e), \mu_{NS}(\dot{e}), \frac{\mu_{PS}(\dot{u})}{(e, \dot{e}, \dot{u})}\right) \quad (6)$$

i.e., each triple $(e, \dot{e}, \dot{u})$ has a membership degree equal to the minimum of $\mu_{PM}(e), \mu_{NS}(\dot{e})$ and $\mu_{PS}(\dot{u})$.

In inference mechanism, the implied fuzzy sets are produced using the max-min composition. In defuzzification, these implied fuzzy sets are combined to provide a crisp value of controller output. The centre of gravity defuzzification method has been used to find out the crisp value of the output. According to COG defuzzification, the crisp value of output is given by

$$\Delta RFM^{crisp} = \frac{\sum_i b_i \int \mu_{conseq,i}}{\sum_i \int \mu_{conseq,i}} \quad (7)$$

Where b_i denote the centre of gravity of the MF of the consequent of rule i. Further, $\int u_{conseq,i}$ denotes the area under the MF $u_{conseq,i}$.

Table 1 Rule base for 7×7 fuzzy logic controller

error	**Δ*error***						
	NB	*NM*	*NS*	*ZE*	*PS*	*PM*	*PB*
NB	*NB*	*NB*	*NB*	*NM*	*NM*	*NS*	*ZE*
NM	*NB*	*NB*	*NM*	*NM*	*NS*	*ZE*	*PS*
NS	*NB*	*NM*	*NM*	*NS*	*ZE*	*PS*	*PM*
ZE	*NM*	*NM*	*NS*	*ZE*	*PS*	*PM*	*PM*
PS	*NM*	*NS*	*ZE*	*PS*	*PM*	*PM*	*PB*
PM	*NS*	*ZE*	*PS*	*PM*	*PM*	*PB*	*PB*
PB	*ZE*	*PS*	*PM*	*PM*	*PB*	*PB*	*PB*

In this control system, the PI system as a forward constraint reference scale the size of fuzzy inputs with error and Δerror, technical engineers need not spend much time on the calibration. Specifically, for non-calibrate points, PI-like fuzzy control systems can revise errors of unknown calibration points adaptively comparing with PI control systems [31].

3. Membership Function Optimisation Scheme

Basically, the MF shape is rarely considered in FLC framework construction for engineering applications, which is often defined as a typical MF pattern. Here, we propose an improved MFO scheme and it uses CA approach to determine MF scalar parameters of an FKBC for AFR management, in which descriptive statistics of relations between fuzzy sets can be visualised conveniently. In Fig. 4, the proposed scheme consists of three main modules: 1) the case starts with to design specialised MF based on weight distribution for the FKBC in the AFR control system. 2) Then designed MF scalar parameters as statistical variables are introduced with engine step gain scenario variables into the CA model, then they are weighted by output results of the FKBC model with each combination of MF pattern and step gain scenario. 3) Through individual assessment, the best MF can be determined then the fuzzy AFR controller with the optimised MF is validated in a production V6 GDI engine with RCP technology.

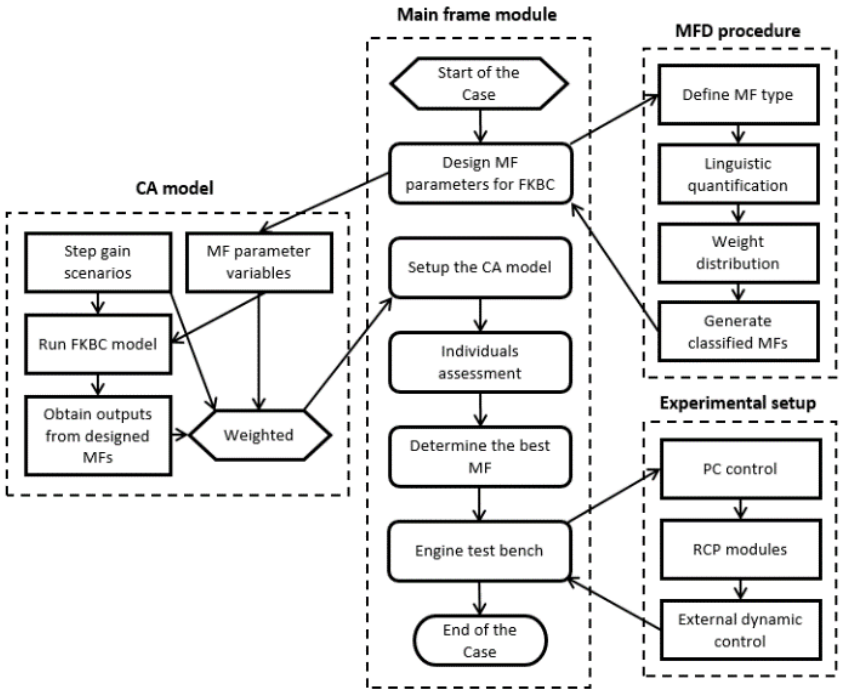

Fig. 4. *The flow chart of MFO scheme.*

3.1. Membership Function Design

In general, typical MF patterns contain Triangular, Gaussian, Bell-shaped, Polynomial and Trapezoidal, which are not enough satisfied to constraint AFR over the different transient change of working operation point. As pointed out by [32], Trapezoidal-shaped MF with higher simplicity is considered to implant into the non-linearity of the controller as the research reference. A function of a vector x and depends on four scalar parameters a, b, c, and d, as given by

$$f_{p,q}(x; a_r, b_r, c_r, d_r) = max\left(min\left(\frac{x-a_r}{b_r-a_r}, 1, \frac{d_r-x}{d_r-c_r}\right), 0\right) \quad (8)$$

Where the parameters $P = [1,2,3]$ is the pth level of top width, $Q = [1,2,3]$ is the qth level of bottom width, $R = [-3,-2,\ldots,2,3]$ is the rth fuzzy set of one MF pattern. a and d locate the "feet" of the trapezoid and the parameters b and c locate the "shoulders." By the way, $b = c$, the MF curve switches to a triangular one. In this case, output MF pattern is considered as standard Triangular type like Fig. 5(a).

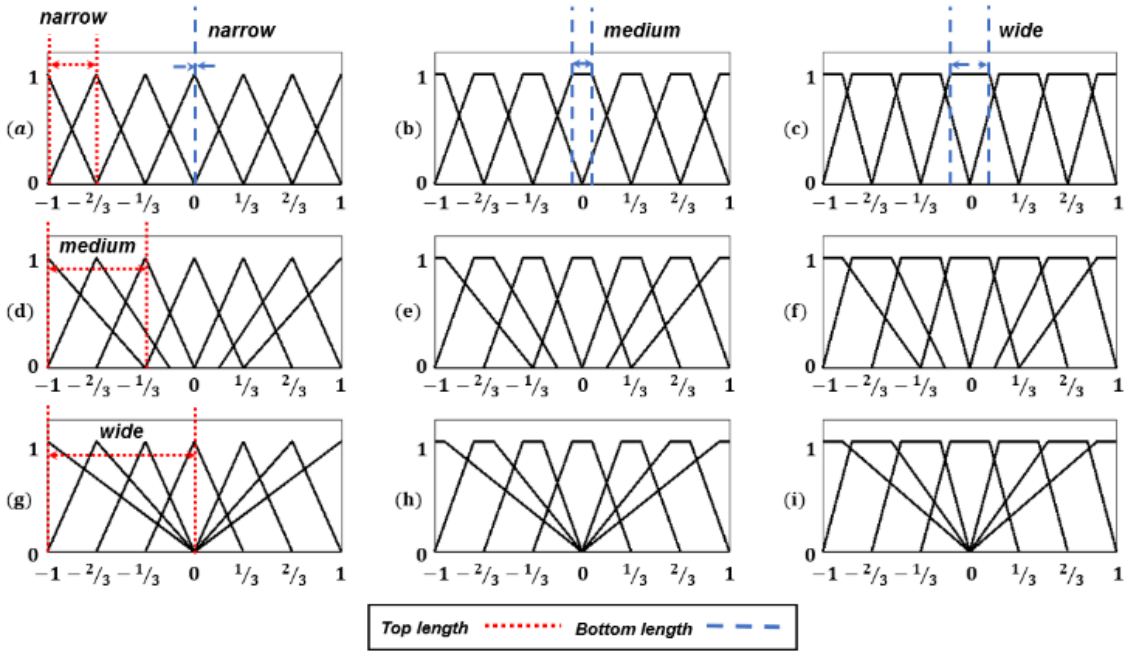

Fig. 5. (a)-(c) *Designed MF patterns with narrow/medium/wide top length and narrow bottom length;* ***(d)-(f)*** *with narrow/medium/wide top length and medium bottom length;* ***(g)-(i)*** *with narrow/medium/wide top length and wide bottom length.*

Table 2 Contingency table for membership value analysis

Step Gain	*Membership Function Pattern*								
	N-N	*N-M*	*N-W*	*M-N*	*M-M*	*M-W*	*W-N*	*W-M*	*W-W*
2%	*0.309*	*0.309*	*0.322*	*0.308*	*0.308*	*0.319*	*0.308*	*0.308*	*0.319*
4%	*0.526*	*0.529*	*0.557*	*0.519*	*0.522*	*0.550*	*0.514*	*0.518*	*0.545*
6%	*0.665*	*0.702*	*0.715*	*0.664*	*0.707*	*0.717*	*0.665*	*0.710*	*0.718*
8%	*0.871*	*0.880*	*0.884*	*0.877*	*0.884*	*0.886*	*0.881*	*0.886*	*0.888*

At the beginning, the unified linguistic quantification of MFD is considered as the prerequisite to build the CA model. Based on the equal weight distribution principle, the MF profile $f_{p,q}$ is classified from top and bottom horizon scalar parameters, which can be described by

$$\begin{cases} a_r = \frac{1}{3}r - \frac{1}{3} \\ b_r = \frac{1}{3}r - \frac{1}{15}(p-1) \\ c_r = \frac{1}{3}r + \frac{1}{15}(p-1) \\ d_r = \frac{1}{3}r + \frac{1}{3} \end{cases} \tag{9}$$

When $r = -3, -2, -1$, the scalar parameter d_r is replaced by

$$d_r = \frac{1}{3}r + \frac{1}{3} + \frac{1}{6}(q-1)(|r|-1) \tag{10}$$

When $r = 1,2,3$, the scalar parameter a_r is replaced by

$$a_r = \frac{1}{3}r - \frac{1}{3} - \frac{1}{6}(q-1)(r-1) \tag{11}$$

According to the above equation, 3×3 MF combinations is generated with classified scalar parameters as Fig. 5. In all cases, the number of crisp space windows is $S = 6 + 1$ and overlapping functional pieces always add up to 1 to remain within a 7 rules context. Top-bottom length combinations of MFs are named "narrow," "medium," and "wide" as well as labelled symbols on the CA main planes.

3.2. Correspondence Analysis

The CA as a priori versus exploratory method is used to investigate the distinction between a priori and exploratory approaches to data analysis. It takes advantage on analysing two non-interval-level variables with three categories, in which CA has been applied for weight method assessment by [33]. Based on discrete variables of step gain and MF pattern, the structure of CA is formatted to visualise the relation between step gain scenarios and MF pattern. Through individual assessment, the MF scalar parameters with its homogenization can be determined to improve AFR control performance.

A. Data Preparation and Normalisation

Based on CA model adaptation conditions, scenarios of throttle opening gains and MF pattern variables are normalised and coded, whereas the dataset thus obtained is organized as a row of table $YA_{i\times j}$ with $i = 9$ rows and $j = 4$ columns, the yielded table is called $YA_{9\times4}$. To define dominant species, the dominance index is weighted by defuzzification result within $[0,1]$. Then, an initial 8% throttle opening with 2%, 4%, 6% and 8% gains is used as references to separately measure signal values of error and Δerror in the FKBC model. Then signal values of error and Δ error input different FIS with 9 MF patterns. After defuzzification process, outputs of different MF patterns are extracted respectively as dominance index in Table 2.

In nine rows, the representative pattern then named 9 species of MF pattern variables as Narrow-Narrow, Narrow-Medium, Narrow-Wide, Medium-Narrow, Medium-Medium, Medium-Wide, Wide-Narrow, Wide-Medium, Wide-Wide. In four columns, there are four levels of throttle opening step including 2%, 4%, 6% and 8% as scenario variables.

B. Definition of Suitability Assessment Standard

The CA is a multivariate extension of weighted averaging ordination to elucidate the relations between MF pattern combinatory and step gains of throttle opening. In this case, the assessment model applied the squared distance of the *j*th row profile from the origin to define MF suitability, which is [34]

$$d_i^2(i,0) = \sum_{m=1}^{M^*} f_{im}^2 \tag{12}$$

Where the larger the distance of the *i*th row profile in the M^* dimensional correspondence plot from the origin, the larger the weighted discrepancy between the profile of the *i*th row category to the average profile of the column categories.

3.3. Testing and Validation Setup

This study is based on Jaguar V6 GDI engine with 3-litre capacity and variable valve timing. The engine test bench and physical specifications as shown in Fig. 6 and Table 3.

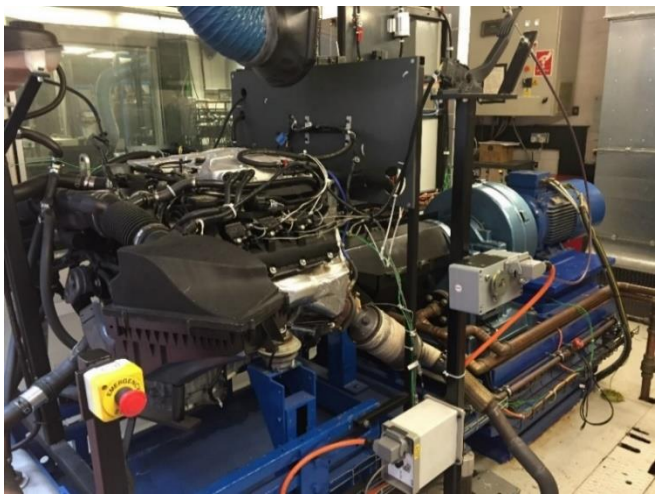

Fig. 6. *Engine test bench: Jaguar V6-3.0 L GDI engine.*

Table 3 Jaguar V6 GDI Engine physical parameters

Parameters	*Value*	*Units*
Bore	*84.5*	*mm*
Stroke	*89*	*mm*
Displacement	*2995*	*cc*
Rod length	*154*	*mm*
Maximum power	*340*	*PS*
Maximum torque	*450*	*Nm*

In RCP control system, there are three main parts involve to the PC control group, RCP modules and external dynamic control system as Fig. 7 shown. The PI-like FKBC model with connection ports of the engine was built by SIMULINK as an original input for INTECRIO. INCA-EIP additional software can be realised on the application of the ES910 module INCA design model characterises.

In this case, ES910 mask ΔRFM(k) signal of ECU then directly sends the bypass signal to the engine test bench through external rapid prototyping. Moreover, there are some signals (e.g. AFR signal) which cannot be collected from sensors on ECU, the ES930 Multi-I/O Module offers several digital and analogy input and output channels for signal recording and output. Then ES930 interchange digital data with the ES910 through daisy chain, in which the AFR signal as the feedback input to the improved Fuzzy AFR controller in the PC terminal. Finally, the optimised control signal skips the ECU's jurisdiction and directly control the GDI engine through ES910. A dyno and AC motor with controllers as engine dynamic control systems mechanically connect with the engine through the crankshaft.

4. Results and Discussion

4.1. Stating Combinatory in the Membership Value Analysis

The CA output analysis is presented cautiously with large summarises as Fig. 8 shown. It is worth noting that the sum of the two relative inertias that are linked to the two main axes is 0.612+0.384=99.6%. This fact explains that there are two dimensions carrying almost entire original information after dimension reduction.

Here, we add a reference frame through the origin $O(0,0)$ and mark critical points of step gains in blue and MF patterns in green to analysis as target groups in Fig. 8(a). The direction of black dotted arrows represents that, with increases of top length, the FIS response at 6-8% step gains become more sensitivity. Then, we link every two of three critical points to establish the orange polygon area. Outside MF patterns are always farther from one or more step gain points relatively, which means defuzzification results of these points are smaller than those of inside points. Meanwhile, these pieces of evidence clearly explain these outside MF patterns are over gentle or aggressive to response step gains of working operation leading to higher overshooting or slow convergence in AFR regulation. Obviously, N-M combination has the more accurate adjustment so that its homogenization can keep trend characteristics of designed MFs while repairing insensitive intervals.

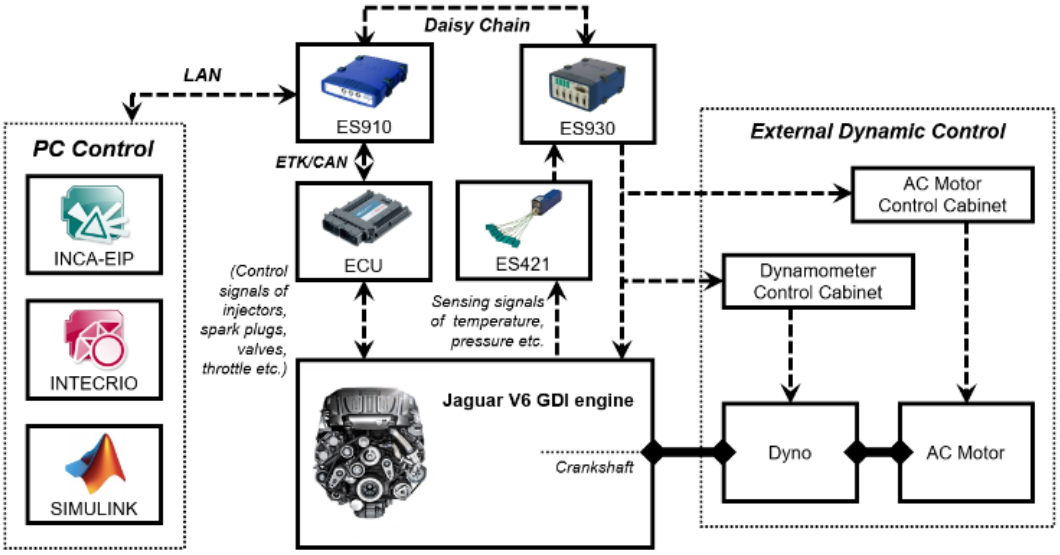

Fig. 7. *The development bench diagram of control strategies.*

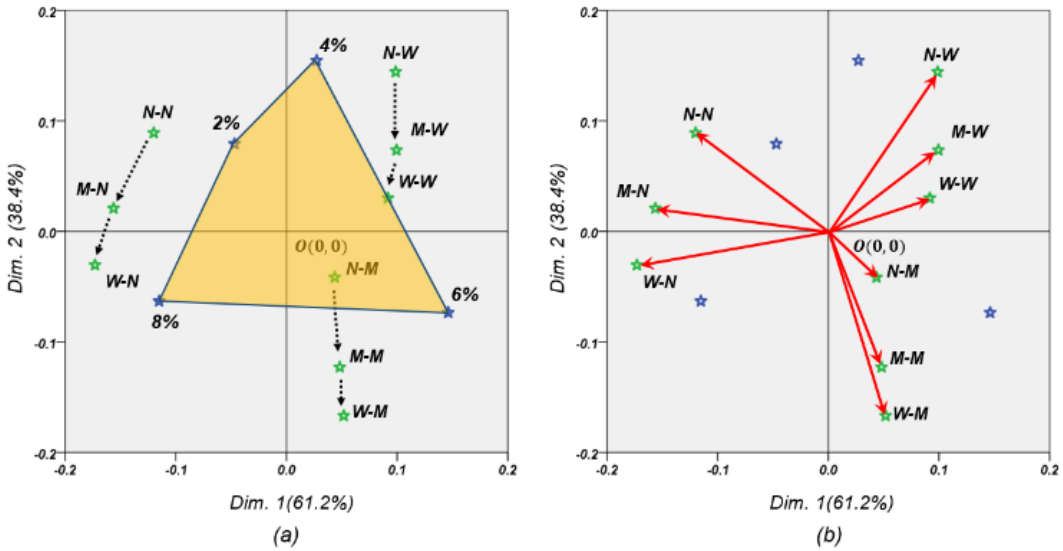

Fig. 8. *CA outputs in the case of the dataset with column (MF pattern) and row (step gain) points, (a) Target group analysis (b) ordination diagram of MF patterns.*

Table 4 The squared distance of MF patterns

MF	*N-N*	*N-M*	*N-W*	*M-N*	*M-M*	*M-W*	*W-N*	*W-M*	*W-W*
d_I^2	*1714.0*	*265.7*	*2304.0*	*1892.3*	*1310.4*	*1169.6*	*2323.2*	*2294.4*	*723.6*

4.2. Membership Function Suitability Assessment

In Table 4, the shortest squared distance from the origin is Narrow-Medium combinatory at 265.7, which means this customised MF profile has the smallest weighted discrepancy to the average profile of throttle opening step gains. It can take an advantage of maximising ΔRFM compensation on AFR control system, especially for stabilising fluctuation caused by transient changes in working scenarios. At last, the CA-based MF pattern with $j = 1, k = 2$ is drawn in Fig 9.

The sensitivity of CA-based MF is compared with two typical MF patterns [28] including Triangular as 'N-N' and Trapezoidal-shaped as 'W-N'. They have the same identical base positions and symmetrical geometry, in which their associated fuzzy control lift surface with 25×25 mesh can demonstrate their gradient changes under different inputs as shown in Fig. 10. The sensitivity of the CA-based MF to the intermediate $[-0.5, 0.5]$ square area of inputs is clearly higher than that of others.

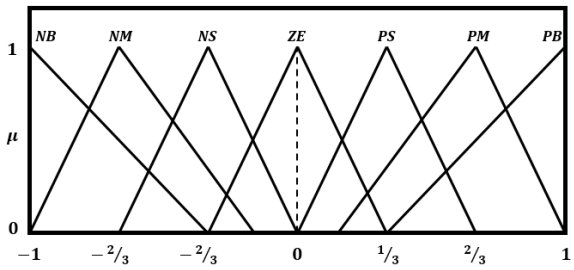

Fig. 9. *The profile of CA-based MF.*

4.3. Real-time Engine Performance

In this study, all experiments are conducted online for testing different existing controllers under the experimental environment with 1500 r/min engine speed fixed by engine

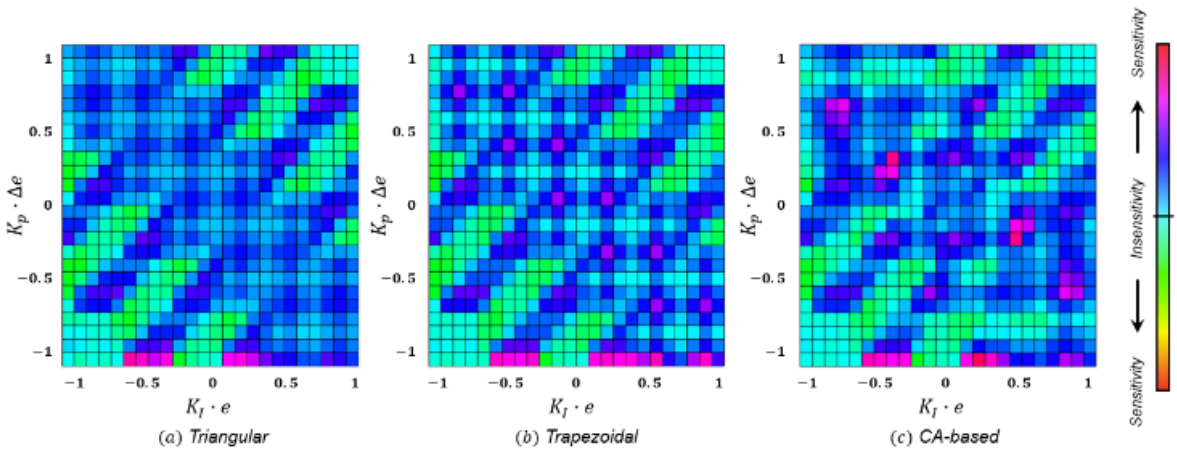

Fig. 10. *Fuzzy control lift surface.*

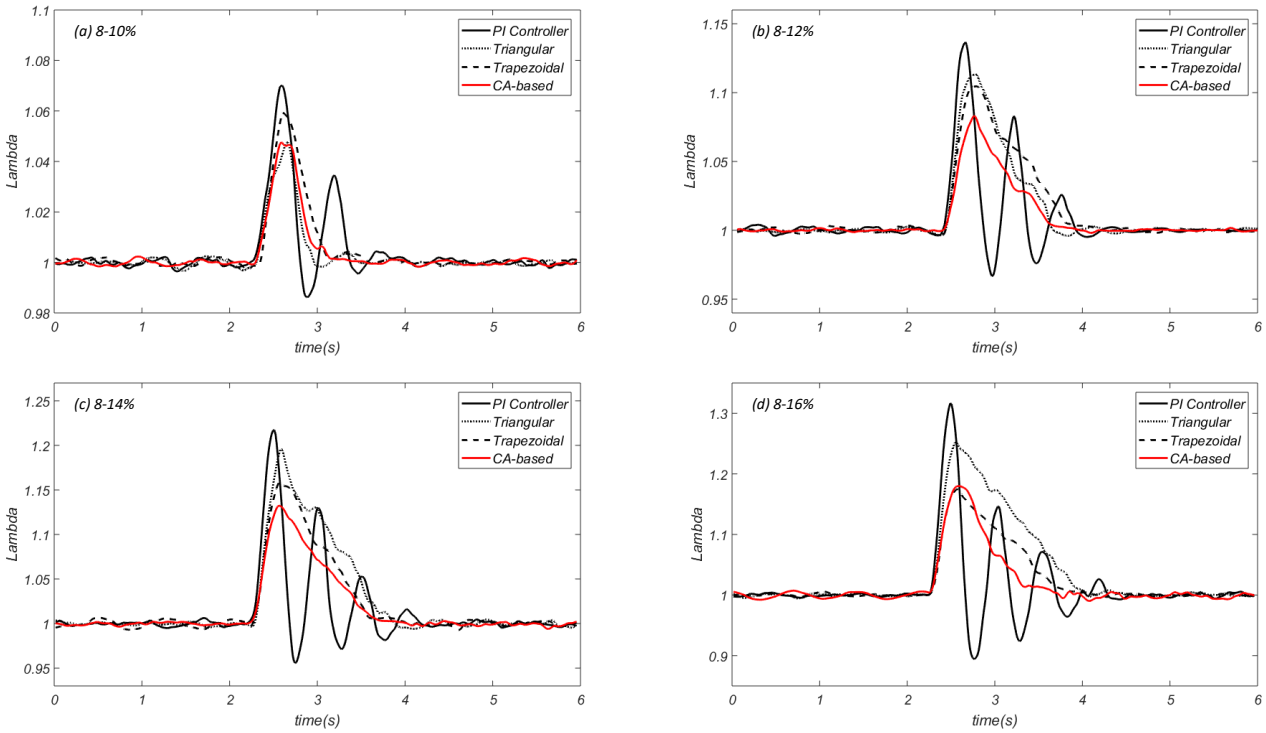

Fig. 11. *The transient responses of AFR under different throttle opening gains.*

dynamic control systems, 8% initial throttle opening and 40% initial relative fuel mass coefficient. Four transient step scenarios with 2%, 4%, 6% and 8% are applied through INCA-EIP in real-time that need to test 4×4=16 times in total. Fig. 11 gives real-time performance comparisons of AFR stabilisation with existing PI and fuzzy controller [9], [10] over different throttle opening gains.

In Fig. 11(a), it can be seen that PI control system has cross-oscillation and severe convergence hysteresis at $\tau_{PI} = 1.058$s with two peaks in this tracking process. Relatively, FLC system avoids overshoot and a large slope cross-oscillation in the process to track $RFM(t)$ reference. Fig. 11(b) shows the comparison results of the AFR regulation at 8-12% throttle opening gain, which are the AFR response curves managed by four methods respectively. Due to the increase of step gains, AFR control performances have varying degrees of deterioration in overshooting and convergence time. Compared to PI controller performance, the FKBC optimised by CA-based MFO reduces 3.2% in overshooting and 27.0% in convergence time. Fig. 11(c) mainly illustrates the advent of the fourth peak in the PI policy leads to a significant increase in convergence time at $\tau_{PI} = 1.875$s. From the trend comparison, all curves are adhering to 8-12% step gain features and Triangular MF continues to deteriorate. In Fig. 11(d), the FKBC optimised by CA-based MFO still restricts overshooting and convergence time within $E_{MFD} = 1.159$ and $\tau_{MFD} = 1.464$s. It has the absolute advantage to control the AFR for reducing exhaust emissions with the high efficiency of TWC.

Here, the integral of the absolute magnitude of error (ITAE) index is introduced that takes advantages of producing smaller overshoots and oscillations [35]. The ITAE criterion is defined as

$$I = \sum_{0}^{\infty} |e| \qquad (13)$$

Performance comparisons of the AFR regulation for GDI engines by using the PI-like FKBC with existing MFs and conventional PI lookup table are summarised in Table 5 with overshooting, convergence time and ITAE.

5. Conclusions

This paper proposes an improved MFO scheme for intelligent fuzzy AFR control of GDI engines with adaptive enhancement, which is validated on a production V6 GDI engine. Conclusions drawn from the research are summarised as follows:

1) According to the CA-based MFO, the customised MF has the more efficient adjustment in with its homogenization can keep trend characteristics of designed MFs while repairing the insensitive interval.
2) A comparison is performed with a commonly PI controller at the absence of PI-like fuzzy control policy. The FKBC optimised by CA-based MFO outperforms the PI controller, in term of both ITAE and convergence time. At 8-10% step gain, the fuzzy logic strategy at most decreases ITAE and convergence time by 50.0% and 52.2% respectively.
3) A comparative study with existing typical MF in the FLC indicates that, at 8-16% step gain, the CA-based one reduces overshooting by 6.9% and convergence time by 24.8% comparing to triangular MF; It is worth mentioning that the FKBC optimised by CA-based MFO can reduce ITAE up to 82% with 8-16% step gain compared to typical MFs.

Table 5 Engine performance comparisons over different scenarios

Step Gain (%)	*Controller Type*	*MF Pattern*	*Overshooting (%)*	*Convergence Time(s)*	*ITAE*
	PI controller	*NA.*	*7.0%*	*1.058*	*5.422*
8-10	*FKBC*	*Triangular*	*4.7%*	*0.695*	*3.625*
	FKBC	*Trapezoidal*	*5.7%*	*0.801*	*4.561*
	FKBC	*CA-based*	*4.1%*	*0.674*	*3.407*
	PI controller	*NA.*	*13.7%*	*1.464*	*10.267*
8-12	*FKBC*	*Triangular*	*10.5%*	*1.173*	*11.704*
	FKBC	*Trapezoidal*	*9.3%*	*1.365*	*12.794*
	FKBC	*CA-based*	*6.9%*	*1.153*	*7.973*
	PI controller	*NA.*	*21.7%*	*1.875*	*16.089*
8-14	*FKBC*	*Triangular*	*16.4%*	*1.426*	*22.991*
	FKBC	*Trapezoidal*	*14.3%*	*1.367*	*19.783*
	FKBC	*CA-based*	*12.3%*	*1.347*	*15.013*
	PI controller	*NA.*	*31.7%*	*2.045*	*23.521*
8-16	*FKBC*	*Triangular*	*22.8%*	*1.827*	*34.654*
	FKBC	*Trapezoidal*	*15.9%*	*1.649*	*21.857*
	FKBC	*CA-based*	*15.9%*	*1.464*	*18.971*

6. References

[1] Boulter, P.G., Barlow, T.J. and McCrae, I.S., 2009. Emission factors 2009: Report 3-exhaust emission factors for road vehicles in the United Kingdom. *TRL Published Project Report*.

[2] Heywood, J., 1988. *Internal combustion engine fundamentals*. McGraw-Hill Education.

[3] Seong, H., Lee, K. and Choi, S., 2013. *Effects of engine operating parameters on morphology of particulates from a gasoline direct injection (GDI) engine* (No. 2013-01-2574). SAE Technical Paper.

[4] Guzzella, L. and Onder, C., 2009. *Introduction to modeling and control of internal combustion engine systems*. Springer Science & Business Media.

[5] Carbot-Rojas, D.A., Escobar-Jiménez, R.F., Gómez-Aguilar, J.F. and Téllez-Anguiano, A.C., 2017. A survey on modeling, biofuels, control and supervision systems applied in internal combustion engines. *Renewable and Sustainable Energy Reviews*, *73*, pp.1070-1085.

[6] Stobart, R.K., Challen, B.J. and Bowyer, R., 2001. *Electronic controls-breeding new engines* (No. 2001-01-0255). SAE Technical Paper.

[7] Rajamani, R., 2011. *Vehicle dynamics and control*. Springer Science & Business Media.

[8] Stone, R., 2012. *Introduction to internal combustion engines*. Palgrave Macmillan.

[9] Saraswati, S., Agarwal, P.K. and Chand, S., 2011. Neural networks and fuzzy logic-based spark advance control of SI engines. *Expert Systems with Applications*, *38*(6), pp.6916-6925.

[10] Jansri, A. and Sooraksa, P., 2012. Enhanced model and fuzzy strategy of air to fuel ratio control for spark ignition engines. *Computers & Mathematics with Applications*, *64*(5), pp.922-933.

[11] Kumar, M. and Shen, T., 2015. Estimation and feedback control of air-fuel ratio for gasoline engines. *Control Theory and Technology*, *13*(2), pp.151-159.

[12] Efimov, D.V., Nikiforov, V.O. and Javaherian, H., 2014. Supervisory control of air–fuel ratio in spark ignition engines. *Control Engineering Practice*, *30*, pp.27-33.

[13] Kumar, M. and Shen, T., 2016. Cyclic model based generalized predictive control of air-fuel ratio for gasoline engines. *Journal of Thermal Science and Technology*, *11*(1), pp.JTST0009-JTST0009.

[14] Boiocchi, R., Gernaey, K.V. and Sin, G., 2016. Systematic design of membership functions for fuzzy-logic control: A case study on one-stage partial nitritation/anammox treatment systems. *Water research*, *102*, pp.346-361.

[15] Rojas, C.A., Rodriguez, J.R., Kouro, S. and Villarroel, F., 2017. Multiobjective fuzzy-decision-making predictive torque control for an induction motor drive. *IEEE Transactions on Power Electronics*, *32*(8), pp.6245-6260.

[16] Nabipour, M., Razaz, M., Seifossadat, S.G. and Mortazavi, S.S., 2016. A novel adaptive fuzzy membership function tuning algorithm for robust control of a PV-based Dynamic Voltage Restorer (DVR). *Engineering Applications of Artificial Intelligence*, *53*, pp.155-175.

[17] Sicre, C., Cucala, A.P. and Fernández-Cardador, A., 2014. Real time regulation of efficient driving of high speed trains based on a genetic algorithm and a fuzzy model of manual driving. *Engineering Applications of Artificial Intelligence*, *29*, pp.79-92.

[18] Huang, Y., Khajepour, A., Khazraee, M., & Bahrami, M., 2017. A comparative study of the energy-saving controllers for automotive air-conditioning/refrigeration systems. *Journal of Dynamic Systems, Measurement, and Control*, 139(1), 014504.

[19] Huang, Y., Khajepour, A., Zhu, T., & Ding, H., 2017. A supervisory energy-saving controller for a novel anti-idling system of service vehicles. *IEEE/ASME Transactions on Mechatronics*, *22*(2), 1037-1046.

[20] Bağiş, A., 2003. Determining fuzzy membership functions with tabu search—an application to control. *Fuzzy sets and systems*, *139*(1), pp.209-225.

[21] Caraveo, C., Valdez, F. and Castillo, O., 2016. Optimization of fuzzy controller design using a new bee colony algorithm with fuzzy dynamic parameter adaptation. *Applied Soft Computing*, *43*, pp.131-142.

[22] Acilar, A.M. and Arslan, A., 2011. Optimization of multiple input–output fuzzy membership functions using clonal selection algorithm. *Expert Systems with Applications*, *38*(3), pp.1374-1381.

[23] Chung, J.H., Pak, J.M., Ahn, C.K., You, S.H., Lim, M.T. and Song, M.K., 2017. Particle filtering approach to membership function adjustment in fuzzy logic systems. *Neurocomputing*, *237*, pp.166-174.

[24] Lee, C.H. and Pan, H.Y., 2009. Performance enhancement for neural fuzzy systems using asymmetric membership functions. *Fuzzy Sets and Systems*, *160*(7), pp.949-971.

[25] Ma, H., Xu, H., Wang, J., Schnier, T., Neaves, B., Tan, C. and Wang, Z., 2015. Model-based multiobjective evolutionary algorithm optimization for HCCI engines. *IEEE Transactions on Vehicular Technology*, 64(9), pp.4326-4331.

[26] Ma, H., Li, Z., Tayarani, M., Lu, G., Xu, H. and Yao, X., 2018. Computational Intelligence Nonmodel-Based Calibration Approach for Internal Combustion Engines. Journal of Dynamic Systems, *Measurement*, and Control, 140(4), p.041002.

[27] Li, Z., Li, J., Zhou, Q., Zhang, Y., & Xu, H., 2018. Intelligent air/fuel ratio control strategy with a PI-like fuzzy knowledge–based controller for gasoline direct injection engines. *Proceedings of the Institution of Mechanical Engineers, Part D: Journal of Automobile Engineering*, DOI: 10.1177/0954407018779180.

[28] Zhang, Y., Zhou, Q., Li, Z., Li, J., & Xu, H., 2018. Intelligent transient calibration of a dual-loop EGR diesel engine using chaos-enhanced accelerated particle swarm optimization algorithm. *Proceedings of the Institution of Mechanical Engineers, Part D: Journal of Automobile Engineering*, 0954407018776745.

[29] Wang, C., Xu, H., Herreros, J.M., Wang, J. and Cracknell, R., 2014. Impact of fuel and injection system on particle emissions from a GDI engine. *Applied Energy*, *132*, pp.178-191.

[30] Jantzen, J., 2013. *Foundations of fuzzy control: a practical approach*. John Wiley & Sons.

[31] Fazzolari, M., Alcala, R., Nojima, Y., Ishibuchi, H. and Herrera, F., 2013. A review of the application of

multiobjective evolutionary fuzzy systems: Current status and further directions. *IEEE Transactions on Fuzzy systems*, *21*(1), pp.45-65.

[32] Jager, R., 1995. *Fuzzy logic in control*. Rene Jager.

[33] Liang, J., Hua, S., Zeng, G., Yuan, Y., Lai, X., Li, X., Li, F., Wu, H., Huang, L. and Yu, X., 2015. Application of weight method based on canonical correspondence analysis for assessment of Anatidae habitat suitability: A case study in East Dongting Lake, Middle China. *Ecological Engineering*, 77, pp.119-126.

[34] Beh, E.J. and Lombardo, R., 2014. *Correspondence analysis: theory, practice and new strategies*. John Wiley & Sons.

[35] Sahu, R.K., Panda, S. and Sekhar, G.C., 2015. A novel hybrid PSO-PS optimized fuzzy PI controller for AGC in multi area interconnected power systems. *International Journal of Electrical Power & Energy Systems*, *64*, pp.880-893.